Pancreatic cancer cells overexpressing interleukin 6 induce T-cell-mediated tumor clearance and durable anti-tumor immune response

Paige C. Arneson-Wissink[1], Alexandra Q. Bartlett[2], Heike Mendez[1], Xinxia Zhu[1], Jessica Dickie[1], Matthew McWhorter[2], Peter R. Levasseur[1], Parham Diba[1], Katelyn T. Byrne[3,4], Gregory D. Scott[5], Robert Eil[2], Aaron J. Grossberg[1, 4, 6]*

[1] Department of Radiation Medicine, Oregon Health & Science University, Portland, OR, 97239, USA
[2] Division of Surgical Oncology, Department of Surgery, Knight Cancer Institute, Oregon Health & Science University, Portland, OR, 97239, USA
[3] Department of Cell, Development, and Cancer Biology, Oregon Health & Science University, Portland, OR, 97239, USA
[4] Brenden Colson Center for Pancreatic Care, Oregon Health & Science University, Portland, OR, 97239, USA
[5] Department of Pathology, Oregon Health & Science University, Portland, OR, 97239, USA
[6] Cancer Early Detection Advanced Research Center, Oregon Health & Science University, Portland, OR, 97201, USA

*__Corresponding Author__: Aaron J. Grossberg, 3181 SW Sam Jackson Park Rd Mail Code L481, Oregon Health and Science University, Portland, OR, 97239, 503-494-9945, grossber@ohsu.edu

Conflict of interest: RE is a paid consultant and conducts ongoing research for Lyell Immunopharma. KTB receives consultation feed from Guidepoint Global and royalties from the University of Pennsylvania for licensed research cell lines. The other authors declare no conflicts.

ABSTRACT

Tumor immune resistance is recognized as a contributor to low survivorship in pancreatic ductal adenocarcinoma (PDAC). We developed a novel murine model of spontaneous PDAC clearance, generated by overexpressing interleukin-6 (IL-6) in orthotopically implanted PDAC cancer cells (OT-PDAC^{IL6}). Circulating IL-6 was 100-fold higher in OT-PDAC^{IL6} than in OT-PDAC^{parental} mice. OT-PDAC^{IL6} tumors were present at 5 days post-implantation, and undetectable by 10 days post implantation. Flow cytometry revealed increased T cells and NK cells, and decreased T regulatory cells in OT-PDAC^{IL6} as compared to OT-PDAC^{parental} tumors. Increased lymphoid aggregates were apparent by histological assessment and may account for elevated T cell content. Antibody-based depletion of $CD4^+$ and $CD8^+$ T cells prevented tumor clearance and significantly reduced survival of OT-PDAC^{IL6} mice. The anti-tumor immune response to OT-PDAC^{IL6} rendered mice immune to re-challenge with OT-PDAC^{parental} tumors. In high concentrations, IL-6 acts in opposition to previously described pro-tumorigenic effects by enhancing the T cell-mediated anti-tumor response to PDAC.

Statement of Significance: Interleukin 6 overexpression in pancreatic ductal adenocarcinoma cells induces T cell-driven tumor clearance that is rapid and durable. Supraphysiologic levels of interleukin 6 are sufficient to drive an anti-tumor immune microenvironment hallmarked by increased lymphoid aggregate formation, increased CD4 T cell abundance, and decreased Treg abundance.

Key words: Interleukin 6, Pancreatic Ductal Adenocarcinoma, T-cell response

INTRODUCTION

Interleukin-6 (IL-6) signaling is associated with reduced survival in patients with pancreatic ductal adenocarcinoma (PDAC), attributed to the promotion of metastasis, tumorigenesis, and cachexia[1-4]. Published literature shows that loss of IL-6 attenuates PDAC development, cachexia onset, and metastasis [5-7]. We previously demonstrated that host intrinsic IL6 signaling was necessary to develop PDAC cachexia[6]. To extend this finding, we sought to ask if IL6 overexpression in cancer cells would be sufficient to restore cachexia in an otherwise IL6 deficient host. We developed stable IL-6 overexpressing PDAC cells ($PDAC^{IL6}$) from the $PDAC^{parental}$ cell line (KxPxCx) [8] using ecotropic retroviral transduction. We found that $PDAC^{IL6}$ cells produced extremely high levels of IL-6 and induced severe cachexia within days of orthotopic implantation (OT-$PDAC^{IL6}$). Despite this, we observed unexpected and dramatic changes in tumor growth dynamics, culminating in complete tumor clearance and long-term, recurrence-free mouse survival. We then pursued a series of studies to understand the mechanistic underpinnings of tumor clearance in our model, focusing on the immune response to high intra-tumoral IL-6. Our work presents a previously undescribed ability for IL-6 to induce T cell-mediated PDAC tumor clearance. Typically, PDAC is associated with an immunosuppressive microenvironment, which limits the efficacy of immunotherapies in treating PDAC [9,10]. Increased T-cell infiltration is associated with improved survival and strategies to increase T-cell activation and infiltration benefit mouse survival in pre-clinical models [11,12]. The work shown here presents IL-6 over-expression as a novel mechanism by which PDAC tumors experience more T cell infiltration and are poised for a favorable anti-tumor immune response.

METHODS

Mouse Studies

Husbandry

C57BL/6J (WT, JAX 000664) mice were purchased from The Jackson Laboratory (Bar Harbor, ME) and maintained in our animal facility. All mice were housed and bred in a dedicated mouse room maintained at 26 °C, 40% humidity, and 12-h light/dark cycle. Mice were provided *ad libitum* access to food and water (5L0D, PicoLab) unless otherwise stated. All mice were 12 weeks of age at experiment start. Sex in each experiment is defined in the figure legends. When single housed, mice were allowed a 7 day acclimation period prior to procedure/study start. All tumor studies followed humane endpoints. All mice were humanely euthanized via cardiac puncture or cervical dislocation under deep isoflurane anesthesia. Mouse studies were conducted in accordance with the NIH Guide for the Care and Use of Laboratory animals, and approved by the Oregon Health & Science University IACUC.

Orthotopic Tumor Implantation

A vial of frozen KPC cells was thawed prior to each implantation, and 1 million cells were implanted in 23 uL of PBS per mouse. All mice were anesthetized with isoflurane, scrubbed with betadine, and a para-midline incision was made in the abdomen to expose pancreas. KPC cells or vehicle (PBS) were injected directly into the pancreatic parenchyma. Pancreas was placed back into position and incision was closed using two sutures (4-0 Polysorb) and two skin staples.

Subcutaneous Tumor Implantation

A vial of frozen KPC cells was thawed prior to each implantation, and 1 or 2 million cells were implanted in 100 uL of PBS per mouse. The mouse's lower right abdomen was shaved, then the needle was inserted near the right 4^{th} mammary gland.

IVIS imaging

Mice were injected with 100 uL of 15 mg/mL D-luciferin potassium salt in DPBS (no Ca, no Mg) (GoldBio, #LUCK-100), then anesthetized with isoflurane. 10 minutes later, a luminescent image and photo were captured. Longitudinal data was analyzed in one batch by normalizing tumor ROI luminescence total counts to average background ROI luminescence total counts.

Antibody-based depletion

Mice were dosed intraperitoneally (IP) with either a combination of CD4 (BioXcell, #BE0003-1) and CD8a (BioXcell, #BE0061) depletion antibodies, or Rat IgG2b isotype control antibody (BioXcell, #BE0090), which were resuspended in InVivoPure ph7.0 Dilution Buffer (BioXcell, #IP0070) per the manufacturer's instructions. First dose was 0.2 mg each antibody per mouse, given IP two days prior to tumor implantation. Following doses were 0.1 mg each antibody per mouse, given IP every 4 days after initial dose.

Cell lines

Growth Conditions and validation

All cells were maintained at 37°C and 5% CO_2 in a humidified incubator, and tested negative in house for mycoplasma using Universal Mycoplasma Detection Kit (30-1012K). *Kras*$^{G12D/+}$, *Tp53*$^{R172H/+}$, *Pdx1-Cre* (KPC) cell line was generously shared by Dr. Elizabeth Jaffee[8,18]. KPC cells were grown on tissue culture-treated dishes in growth media consisting of RPMI (Gibco) with 10% FBS (Corning) and 1% penicillin/streptomycin (Gibco).

Engineered KPC

KPC cells expressing the surface marker Thy1.1 (CD90.1) with blasticidin resistance (BSR), IL-6 with puromycin resistance, and luciferase with hygromycin resistance, were generated from our stock of KPC cells (female) described above. IL-6 sequence was codon-optimized for efficient expression (**Figure S9**). Platinum-E ecotropic packaging cells were transfected with

plasmid DNA encoding MSGV-Thy1.1, MSGV-IL6-Puro, or MSGV-Luciferase as described previously[19]. Retroviral supernatants were spiked with 2ug/mL polybrene and were mixed 1:1 with fresh media before adding to 6-well tissue culture treated plates. Cells were spun at 2000g for 90min, 32C, no brake. Cells were then incubated at 37C for 48 hours before washing off the viral supernatant and adding DMEM media (Gibco) supplemented with 10% FBS (Corning). Two days later, KPC cells were placed in complete DMEM media containing puromycin (5ug/mL) and/or blasticidin (5ug/mL) and/or hygromycin (500 ug/mL) to select for transduced cells. Following antibiotic selection, successful transduction was confirmed via flow cytometry staining for Thy1.1. KPC-CD90.1, KPC^{IL6}, and KPC^{LUC} cells were implanted for OT-PDAC as described for parental KPC cells. Continued culturing of engineered cells was done in selection media described.

Flow cytometry

Brefeldin A injections: For intracellular cytokine staining for flow cytometry, we followed previously published protocols for golgi transport blockade[20]. Briefly, each mouse received 100ug Brefeldin A (Selleckchem) injected retro-orbitally 5 hours prior to tissue collection.

Sample preparation

We collected tumors from mice 5 days post implantation, and tumors were weighed, then placed in PBS on ice. Tumor tissue was minced and digested (7). After dissociation, we strained tumor suspension through at 100 um filter, and performed ACK lysis. We collected spleens from mice at the endpoint specified. Spleens were pressed through a 70 um filter, rinsed with PBS, pelleted at 1500 RPM for 5 minutes, and lysed with ACK lysis.

Staining

We stained samples with live/dead stain (1:2000) and surface protein antibodies (1:200 each),

and incubated for 20 minutes room temperature (**Table S3**). After staining, we washed samples with FACS buffer and pelleted. For intracellular staining (Foxp3), we fixed and permeabilized cells with 4% paraformaldehyde (BD Cytofix/Cytoperm), washed cells, and then resuspended cells in antibody diluted 1:200 in permeabilization buffer (BD Perm/Wash) with overnight incubation at 4C . The next day we washed and resuspended cells with FACS buffer prior to analysis.

Instrumentation and analysis

All samples were analyzed in the OHSU Flow Cytometry Shared Resource using the Cytek Aurora flow cytometer (Cytek Biosystems), data was analyzed in FlowJoTM v10.8.1. Samples were first gated according to size and single cells, then all live cells were captured. The live population was gated on CD45+ cells to capture all leukocytes. To identify T cells, leukocytes were gated on CD90.2 then sub-gated for CD4+ or CD8+ cells. The CD4+ T cell population was gated on Foxp3 to assess T regulatory cells. Natural killer (NK) cells were sub-gated from the parental CD45+ gate. All NK1.1+ cells were captured, and then divided by expression of CD90.2 to classify as NK (conventional, CD90.2-) or NK T cells (CD90.2+).

Histology

Pancreas/tumor tissue was fixed overnight in 4% PFA, then stored in 70% ethanol. Tissues were paraffin embedded, sectioned, and hematoxylin and eosin (H&E) stained by the OHSU Histopathology Shared Resource. Tumor tissue was sectioned in 5um slices at levels 50 um apart. H&E stained tumor cross-sections were evaluated by a board-certified gastrointestinal pathologist. All samples were blinded during sectioning/staining and during evaluation. 3-5 depths of tissue were qualitatively assessed per mouse. For day 5 tumor samples, 2 depths of

tissue were quantified per mouse and averaged together. For day 12 tumor samples, 1 section was quantified.

Immunofluorescent staining and quantification

Pancreas/tumor tissue was dissected, transferred to BD Cytofix/Cytoperm diluted to 1% PFA, and kept at 4C overnight. Tissue was then transferred to 30% sucrose in PBS and kept at 4C overnight. Tissue was then washed twice in PBS before embedding in OCT media (Sakura). Tissue was cut at 8 um onto superfrost plus slides and stored at -80C until staining. To stain, slides were washed with PBS, blocked with 2.5% BSA 0.3% TritonX in PBS for one hour, stained with pre-conjugated antibodies (**Table S3**) for 1h, washed with PBS, quenched with TrueView Autofluorescence Quench kit (Vector, SP-8400) 2-5 min, stained with DAPI diluted 1:1000 for 10 min, and mounted with Vectashield Vibrance mounting medium (Vector, H-1700). Whole tissue sections were imaged on a Zeiss Axio Scan 7 at 20x magnification. Two tissue sections at least 344 um apart were assessed per sample. All images were blinded prior to annotation and analysis. In QuPath (V0.5.1), areas of tumor, as defined as PanCK positive, and stroma, as defined as PanCK negative abnormal tissue, were annotated. Adjacent tissue sections were stained with H&E and used as reference for areas of stroma. Annotations were made using only the DAPI and PanCK stains. After annotation, $CD3^+$ cells ($CD3^+$, $DAPI^+$, PanCK-) were manually counted in stroma and tumor areas. Final counts were normalized to total area of stroma or tumor annotation.

Plasma analytes

Plasma was collected, snap frozen in liquid nitrogen, and stored at -80ºC. Plasma concentrations of IL-6 (Biolegend) were measured using ELISA, and read on a plate reader (BioTek).

Quantitative real-time polymerase chain reaction (qPCR)

We isolated RNA from cell pellets or tissue samples using the E.Z.N.A. Total RNA Kit I (Omega BioTek), and we prepared cDNA using a high-capacity cDNA reverse transcription kit (Applied Biosystems). qPCR was run on the ABI 7300 (Applied Biosystems), using TaqMan Fast Advanced PCR master mix (Applied Biosystems) or SYBR Green master mix (Applied Biosystems). Relative expression was calculated using the $\Delta\Delta C_t$ method. To confirm the presence/absence of *Il6 transgene* in tumor-implanted mice, we performed 30 cycles of qPCR on the ABI7300, followed by running the PCR product on a 3% ethidium bromide gel to determine the presence of a band at the expected size of 131 bp. Primers/probes are listed in **Table S2**.

Statistical Analysis

Specific statistical tests and sample sizes for each study are indicated in the figure legends. Error bars in the figures show SEM. Statistical analyses were performed using GraphPad Prism (version 9; GraphPad Software Inc) or JMP Pro (version 16; SAS Institute Inc), and graphs were built using GraphPad Prism (GraphPad Software Inc) statistical analysis software. P values are two-sided, with values less than 0.05 regarded as statistically significant.

Data Availability

Further information and resources, including plasmid sequences, engineered KPC cells, and raw data, will be shared upon reasonable request to Aaron J. Grossberg (grossber@ohsu.edu).

RESULTS

Tumor-specific IL6 overexpression induces spontaneous tumor clearance and cachexia recovery. We developed PDAC^{IL6} and control-transduced PDAC$^{CD90.1}$ cells from the

PDAC^{parental} (KxPxCx, [8]) using ecotropic retroviral transduction. Histological assessments of tumors showed that both OT-PDAC^{IL6} and OT-PDAC^{parental} developed poorly differentiated, infiltrative carcinoma by five days (**Figure 1A-C**). OT-PDAC^{IL6} tumors were slightly smaller in mass and histological area than OT-PDAC^{parental} tumors (**Figure 1C-D**). By 12 days, OT-PDAC^{parental} and OT-PDAC$^{CD90.1}$ mice had reached humane euthanasia endpoint, with carcinoma covering approximately 80% of total tissue area, in contrast, OT-PDAC^{IL6} tissue was completely devoid of tumor, and mice had regained all bodyweight lost during tumor growth (**Figure 1B, D-E, I, Figure S1A-D, Table S1**). We confirmed this result molecularly using qPCR for the codon-optimized *Il6* transgene, which was not detected in OT-PDAC^{IL6} whole pancreas tissue after five days (**Figure 1F, Figure S2A-D**). While lung and liver metastases were detected by *Il6* transgene qPCR at five days, there were no metastases detected at 12 days (**Figure S3A-D**). Spontaneous tumor clearance also occurred when PDAC^{IL6} cells were implanted subcutaneously, indicating that the phenomenon is not specific to intrapancreatic administration (**Figure S4A-C**). IL-6 overexpressing models generated from alternative PDAC cell lines also displayed increased survival and decreased tumor burden relative to parental lines, although we did not observe complete tumor resolution in the other cell lines (**Figure S5A-F**).

To assess the cachexia phenotype and general mouse health, we measured plasma IL-6, a known contributor to cachexia development. OT-PDAC^{parental} plasma IL-6 levels were in line with previously published values, while OT-PDAC^{IL6} levels reached 100-fold higher levels at day 5, followed by undetectable levels at later time points (**Figure 1G**) [3,6]. Spleens from OT-PDAC^{IL6} mice were significantly enlarged, consistent with systemic inflammation elicited by high circulating IL-6 levels (**Figure 1H**). High plasma IL-6 and peak tumor burden also

associated with decreased body mass, which recovered with the normalization of IL-6 (**Figure 1I**). Gross muscle and adipose tissue mass trended downward at five days and were significantly decreased at 12 days, reflecting a delay in tissue recovery as the tumor resolves and body mass returns to baseline (**Figure 1J-L**). Collectively, these data show that IL-6 overexpression in PDAC cells leads to severe wasting, followed by spontaneous tumor resolution.

OT-PDAC^{IL6} induces lymphocytic anti-tumor immune response. We hypothesized that the extreme levels of IL-6 generated in the pancreas of OT-PDAC^{IL6} mice facilitated immune-mediated tumor clearance. We used flow cytometry to evaluate the immune profile of OT-PDAC^{IL6} and OT-PDAC^{parental} tumors and discovered that pancreata bearing OT-PDAC^{IL6} tumors were enriched with CD4^{+} T cells and Natural Killer (NK) cells, while Foxp3^{+} T-regulatory cells were decreased (**Figure 2A-E, Figure S6A-C**). Because increased tumor-infiltrating lymphocytes are associated with improved outcomes and therapeutic efficacy, we next assessed the localization of T cells relative to tumor[12]. By immunofluorescent staining, we found that OT-PDAC^{parental} and OT-PDAC^{IL6} mice had equal densities of CD3^{+} T cells in both tumor-associated stroma and tumor nests (**Figure 2F-H**). These data were initially contradictory to the flow cytometry data. However, upon histological assessment, we found that OT-PDAC^{IL6} pancreata exhibited a significantly greater number of tumor-associated lymphoid aggregates (**Figure 2I-J**). In PDAC, lymphoid aggregate formation is associated with improved survival[13,14]. In OT-PDAC^{IL6} mice, the lymphoid aggregates were often near, but not necessarily located within the tumor stroma, which accounts for the differences between our flow cytometry and immunofluorescence data. In summary, locally high IL-6 induces accumulation of lymphoid aggregates, increased CD4^{+} T cells, and decreased Foxp3^{+} T

regulatory cells. These conditions favor the hypothesis that tumor clearance occurs via an anti-tumor T cell response.

T cells are necessary for OT-PDAC^{IL6} tumor clearance. Based on our flow cytometry analysis, we hypothesized that T cells are necessary for OT-PDAC^{IL6} tumor clearance, which we tested using CD4 and CD8 depletion antibodies, compared to IgG control treatment. Mice received antibody injections two days before tumor implantation and every four days following. We followed humane endpoints for the CD4/CD8-depleted group, which reached euthanasia criteria at 8-11 days post-implantation (**Figure 3A**). We euthanized all sham and IgG-treated mice when all CD4/CD8-depleted mice were euthanized, although they were healthy at the time. We used a second engineered cell line, PDAC$^{IL6\text{-}LUC}$, which expressed luciferase, to measure tumor burden over time. Both OT-PDAC$^{IL6\text{-}LUC}$ longitudinal data and OT-PDAC^{IL6} endpoint tumor mass data show that CD4/CD8 depletion prevents tumor clearance (**Figure 3B-C, Figure S7A-D**). Histological evaluation by a board-certified pathologist found tumor present in 10/10 CD4/CD8-depleted mice and in 1/8 IgG control mice (**Figure 3D**). This was supported by *Il6*-transgene qPCR data and plasma IL-6 levels, which showed no elevation of IL-6 in 6/8 IgG-treated PDAC mice (**Figure 3E-F**). We conclude that CD4 and CD8 T cells are necessary for OT-PDAC^{IL6} tumor clearance.

Because we previously saw recovery of wasting phenotypes in OT-PDAC^{IL6} mice as the tumor resolved, we also investigated cachexia resolution in T cell-depleted mice. CD4/CD8 depletion prevented body mass recovery and led to sustained muscle wasting, as evidenced by decreased muscle mass and increased atrophy-related gene expression (*Trim63, Fbxo32*) (**Figure 3G-I**). The recovery in wasting is therefore directly associated with immune-mediated tumor clearance.

OT-PDAC^{IL6} induces a durable T cell response to OT-PDAC^{Parental} tumors. Given the dependency of the anti-OT-PDAC^{IL6} response on T cells, which are known to elicit immunologic memory, we hypothesized that OT-PDAC^{IL6} tumors would generate a durable immune response that would protect mice in the case of a second tumor exposure. We first tested this hypothesis in a cohort of mice that had recovered from sham surgery or OT-PDAC^{IL6} for over two months and rechallenged mice with OT-PDAC$^{parental\text{-}LUC}$ (luciferase-expressing) at 76 days after initial surgery (**Figure 4A**). Sham-recovered mice implanted with PDAC$^{parental\text{-}LUC}$ reached euthanasia criteria 13-14 days post rechallenge implantation. There were no deaths during rechallenge in the OT-PDAC^{IL6}-recovered group (**Figure 4B**). Tumor burden measured longitudinally by IVIS and terminally (in sham-recovered mice only) revealed significant tumor growth only in sham-recovered mice (**Figure 4C-D, Figure S8A**). Sham-recovered mice also lost more body mass than OT-PDAC^{IL6}-recovered mice during rechallenge (**Figure 4E**). These data indicate that the potent anti-tumor immune response elicited by high concentrations of IL-6 is durable and not dependent on coincident supraphysiologic IL-6 levels. We then used CD4/CD8 antibody depletion to determine whether the tumor clearance during rechallenge was indeed T-cell-mediated. In this study, all mice recovered from OT-PDAC^{IL6} for 26 days before starting antibody treatment and were given sham surgery or implanted with OT-PDAC^{parental} tumors on day 28. We monitored mice for 12 days, until CD4/CD8-depleted mice reached humane euthanasia criteria (**Figure 4F**). We confirmed that clearance of the rechallenge OT-PDAC^{parental} tumor is dependent on T cells, which were effectively depleted by the antibody treatment (**Figure 4G-I**). Furthermore, we confirmed that CD4/CD8-depletion does not result in outgrowth of potentially covert PDAC^{IL6} cells, as there was no tumor present in the OT-PDAC^{IL6}-recovered, sham-rechallenged,

CD4/CD8-depleted mice (**Figure 4G**). These data show that the T cell response induced by OT-PDAC^{IL6} provides durable protection against molecularly similar PDAC tumor growth.

DISCUSSION

Our model of PDAC IL-6 overexpression induces a robust, rapid, and durable anti-tumor T cell response that is accompanied by rapid and severe wasting, which recovers as the tumor is cleared. Although IL-6 is traditionally viewed as a negative actor in pancreatic cancer [1-4], we provide evidence that supraphysiologic levels of IL-6 are sufficient to induce an anti-tumor immune landscape in the pancreas characterized by: increased lymphoid aggregate formation, elevated CD4$^+$ T cells, and decreased Foxp3$^+$ Treg cells.

Unlike cancer types that are now successfully treated with immunotherapy, survival rates for PDAC patients have increased very slowly over the past decade[15]. PDAC is highly immunosuppressive, causing immunotherapies, such as checkpoint blockade, to be ineffective clinically [16]. Previous work indicates that enhancing T-cell activation using exogenous agents, such as agonistic anti-CD40 antibody, improves response to checkpoint blockade therapies and PDAC tumor regression[9]. Our work provides a basis for pursuing IL-6 as an alternative method to improve T-cell response.

Our work raises a fundamental contradiction regarding the role of IL-6 in PDAC. We propose that the effect of IL-6 on PDAC growth is pleiotropic and concentration-dependent. At low concentrations, IL-6 aids tumor development via signaling directly on neoplastic cells to drive transformation and growth. At supraphysiologic concentrations seen in OT-PDAC^{IL6} tumor-bearing mice, IL-6 stimulates an anti-tumor immune response. Circulating levels are approximately 100 times higher than what we detect in OT-PDAC^{parental} mice, and we presume

that local concentrations in the pancreas are even higher. We can infer that tumor-derived IL-6 is the initiating signal for T-cell accumulation and eventual tumor clearance, however, the precise manner in which IL-6 mediates this remains unknown. In addition to increased numbers of tumor-infiltrating T cells, we detected increased NK cells, increased neutrophils, and decreased Treg cells intratumorally. It is possible that IL-6, which is a known immunomodulatory cytokine, impacts multiple cell populations simultaneously to orchestrate an anti-tumor immune microenvironment[17].

Although we initially developed the OT-PDAC^{IL6} model to study the effects of IL-6 on cancer cachexia, we have now discovered a novel role for IL-6 to induce a robust anti-tumor T-cell response in PDAC. Our data support the widely-accepted notion that IL-6 induces acutely negative effects, as evidenced by rapid body mass loss of 10-15% in OT-PDAC^{IL6} mice (**Figure 1H**). From a reductionist perspective, this model will open doors to understanding IL-6-mediated T-cell activation in PDAC and the intricacies of cachexia resolution after PDAC tumor clearance. Future work will focus on identifying the immune subpopulations that integrate IL-6 signaling into a T-cell response, with the goal of identifying targetable drivers of the anti-tumor response. This will be clinically meaningful as leaning on high-dose IL-6, a known driver of cachexia, is likely dangerous for already vulnerable patients with PDAC.

ACKNOWLEDGEMENTS

We thank all members of the Aaron Grossberg, Robert Eil, and Katelyn Byrne labs for their helpful discussion and suggestions. We also acknowledge the expert technical assistance by staff in the Advanced Multiscale Microscopy Shared Resource and Histopathology Shared Resource. Author contributions are: Conceptualization, PCAW, AQB, RE, and AJG. Methodology, PCAW, AQB, KTB, RE, AJG. Validation, PCAW, AQB, HM, XZ, JD, MM, PRL,

PD. Formal Analysis, PCAW, AQB, HM, XZ, JD, PD, GDS, AJG. Investigation, PCAW, AQB, HM, XZ, JD, MM, PRL, PD, MM, GDS. Writing—Original Draft, PCAW. Writing – Review and Editing, PCAW, AQB, KTB, RE, AJG. Visualization, PCAW, AQB, PD. Supervision, RE, AJG. Project Administration, RE, AJG. Funding Acquisition, RE, AJG. All authors approved this manuscript.

Funding: This work was supported by the National Cancer Institute (AJG: K08CA245188, R37CA280692, R01CA264133; RE: K08CA256179), the Brenden Colson Center for Pancreatic Care, the Oregon Pancreas Tissue Registry, the Histopathology Shared Resource for pathology studies (University Shared Resource Program at Oregon Health and Sciences University and the Knight Cancer Institute (P30 CA069533 and P30 CA069533 13S5)), the OHSU Flow Cytometry Shared Resource (OHSU Knight Cancer Institute NCI Cancer Center Support Grant P30CA069533), and the Advanced Multiscale Microscopy Shared Resource (OHSU Knight Cancer Institute, NIH P30 CA069533). RE was also supported by grants from the American Association of Cancer Research, ASCO, and Pancreatic Cancer Action Network.

REFERENCES

1 Corcoran, R. B. *et al.* STAT3 plays a critical role in KRAS-induced pancreatic tumorigenesis. *Cancer research* **71**, 5020-5029 (2011).

2 Suh, S.-Y. *et al.* Interleukin-6 but not tumour necrosis factor-alpha predicts survival in patients with advanced cancer. *Supportive Care in Cancer* **21**, 3071-3077 (2013).

3 Rupert, J. E. *et al.* Tumor-derived IL-6 and trans-signaling among tumor, fat, and muscle mediate pancreatic cancer cachexia. *Journal of Experimental Medicine* **218**, e20190450 (2021).

4 Razidlo, G. L., Burton, K. M. & McNiven, M. A. Interleukin-6 promotes pancreatic cancer cell migration by rapidly activating the small GTPase CDC42. *Journal of Biological Chemistry* **293**, 11143-11153 (2018).

5 Flint, T. R. *et al.* Tumor-induced IL-6 reprograms host metabolism to suppress anti-tumor immunity. *Cell metabolism* **24**, 672-684 (2016).

6 Arneson-Wissink, P. C. *et al.* Hepatic signal transducer and activator of transcription-3 signalling drives early-stage pancreatic cancer cachexia via suppressed ketogenesis. *Journal of Cachexia, Sarcopenia and Muscle* (2024).

7 Zhang, Y. *et al.* Interleukin-6 is required for pancreatic cancer progression by promoting MAPK signaling activation and oxidative stress resistance. *Cancer research* **73**, 6359-6374 (2013).

8 Foley, K. *et al.* Semaphorin 3D autocrine signaling mediates the metastatic role of annexin A2 in pancreatic cancer. *Science signaling* **8**, ra77-ra77 (2015).

9 Winograd, R. *et al.* Induction of T-cell immunity overcomes complete resistance to PD-1 and CTLA-4 blockade and improves survival in pancreatic carcinoma. *Cancer immunology research* **3**, 399-411 (2015).

10 Beatty, G. L., Eghbali, S. & Kim, R. Deploying immunotherapy in pancreatic cancer: defining mechanisms of response and resistance. *American Society of Clinical Oncology Educational Book* **37**, 267-278 (2017).

11 Byrne, K. T. & Vonderheide, R. H. CD40 stimulation obviates innate sensors and drives T cell immunity in cancer. *Cell reports* **15**, 2719-2732 (2016).

12 Ino, Y. *et al.* Immune cell infiltration as an indicator of the immune microenvironment of pancreatic cancer. *British journal of cancer* **108**, 914-923 (2013).

13 Hiraoka, N. *et al.* Intratumoral tertiary lymphoid organ is a favourable prognosticator in patients with pancreatic cancer. *British journal of cancer* **112**, 1782-1790 (2015).

14 Sautès-Fridman, C., Petitprez, F., Calderaro, J. & Fridman, W. H. Tertiary lymphoid structures in the era of cancer immunotherapy. *Nature Reviews Cancer* **19**, 307-325 (2019).

15 Siegel, R. L., Miller, K. D., Wagle, N. S. & Jemal, A. Cancer statistics, 2023. *CA: a cancer journal for clinicians* **73**, 17-48 (2023).

16 Hilmi, M. *et al.* The immunological landscape in pancreatic ductal adenocarcinoma and overcoming resistance to immunotherapy. *The Lancet Gastroenterology & Hepatology* (2023).

17 Soler, M. F., Abaurrea, A., Azcoaga, P., Araujo, A. M. & Caffarel, M. M. New perspectives in cancer immunotherapy: targeting IL-6 cytokine family. *Journal for ImmunoTherapy of Cancer* **11** (2023).

18 Michaelis, K. A. *et al.* Establishment and characterization of a novel murine model of pancreatic cancer cachexia. *Journal of cachexia, sarcopenia and muscle* **8**, 824-838 (2017).

19 Eil, R. *et al.* Ionic immune suppression within the tumour microenvironment limits T cell effector function. *Nature* **537**, 539-543 (2016).

20 Liu, F. & Whitton, J. L. Cutting edge: re-evaluating the in vivo cytokine responses of CD8+ T cells during primary and secondary viral infections. *The Journal of Immunology* **174**, 5936-5940 (2005).

FIGURES AND FIGURE LEGENDS

Figure 1

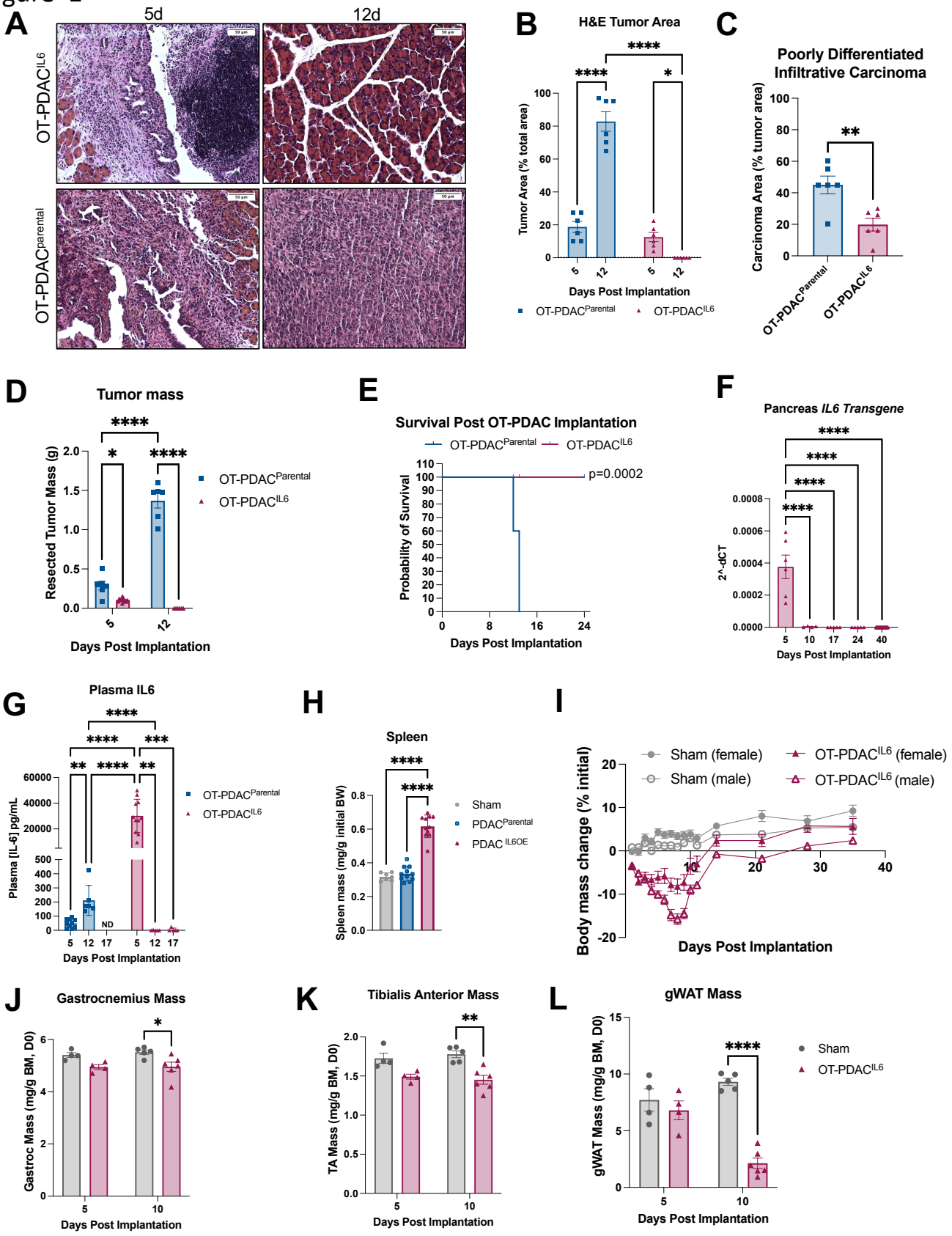

Figure 1: Tumor-specific IL6 overexpression induces spontaneous tumor clearance and cachexia recovery. (A) Representative pancreas cross sections at 5 (left) and 10 days (right) from OT-PDAC^{IL6} (top) and OT-PDAC^{parental} (bottom) tumor implantation. Scale bars represent 50 um (top) and 100 um (bottom). (B) Tumor area as a percent of total tissue area at 5 and 12 days, quantified by board-certified pathologist. (C) Percentage of tumor area classified as poorly-differentiated, infiltrative carcinoma at 5 days by board-certified pathologist. (D) Tumor mass at 5 and 12 days. (B-D) N = 3 male, 3 female mice per group. (E) Survival comparison of OT-PDAC^{Parental} and OT-PDAC^{IL6}. OT-PDAC^{IL6} were euthanized for study endpoint at 24 days, but had not reached humane euthanasia criteria. N = 4 female, 6 male PDAC^{IL6}, 1 female, 4 male PDAC^{parental} mice. Statistically tested with Log-rank (Mantel-Cox) test. (F) Expression of *Il6 transgene* expression, measured by qPCR at 5 (N = 3 male, 3 female), 10 (N = 6 male), 17 (N = 3 male, 2 female), 24 (N = 3 male, 2 female), and 40 (N = 16 male, 16 female) days. Statistically tested with One-way ANOVA with Tukey correction for multiple comparisons. (G) Plasma IL6 measured by ELISA at 5 (N = 10 male PDAC^{Parental}, 11 male PDAC^{IL6}), 12(N = 3 male, 3 female PDAC^{Parental}, 3 male, 2 female PDAC^{IL6}), and 17 (N = 2 male, 3 female PDAC^{IL6}) days. Statistically tested with 2-way ANOVA main effects only with Tukey correction for multiple comparisons. (H) Spleen mass at 5 days. N = 6 male mice per group. (I) Body mass change as a percentage of initial body mass over time. N = 8 male, 8 female mice per group. Statistically tested with 3-way ANOVA. $p<0.0001$ for Time, Sex, Tumor Status, Time x Sex, Time x Tumor Status. $p=0.0002$ for Sex x Tumor Status. $p= 0.2900$ for Time x Sex x Tumor Status. (J) Gastrocnemius muscle mass normalized to initial body mass. (K) Tibialis anterior muscle mass normalized to initial body mass. (L) gonadal white adipose tissue (gWAT) mass normalized to initial body mass. (J-L) 5d N = 1 female, 3 male mice per group. 10d N = 6 male PDAC, 5 male sham mice. Error bars represent SEM. Unless otherwise noted, 2x2 studies were statistically tested with a full effects model 2-way ANOVA and Sidak multiple comparisons test. 2-group analysis tested with unpaired t-test. **** $p<0.0001$, *** $p<0.001$, ** $p<0.01$, * $p<0.05$.

Figure 2

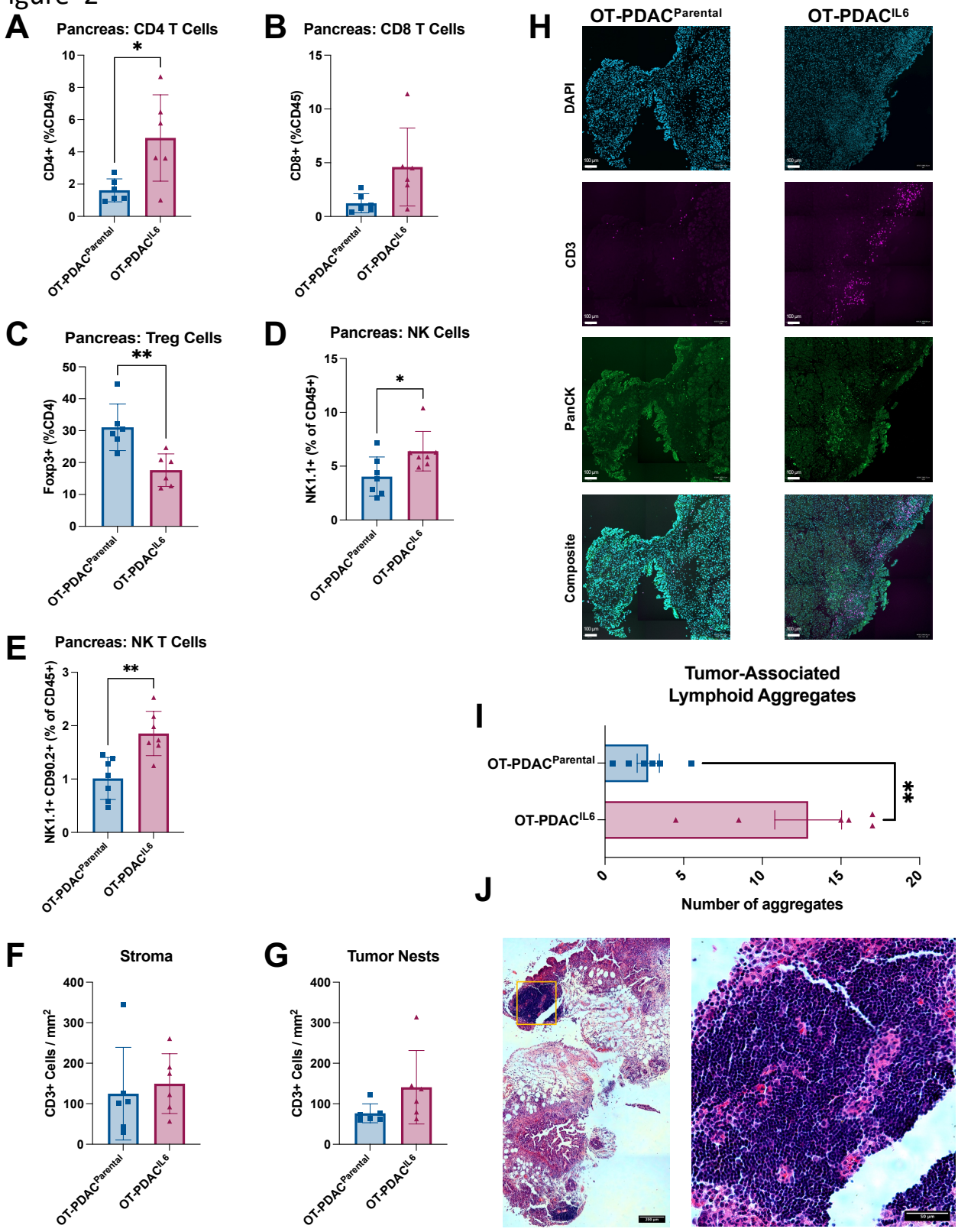

Figure 2: OT-PDAC^{IL6} induces lymphocytic anti-tumor immune response. (A-E) Intra-tumoral immune cell populations from pancreas at 5 days: (A) CD4$^+$ T cells, (B) CD8$^+$ T cells, (C) Foxp3$^+$ T regulatory cells, (D) NK1.1$^+$ Natural Killer cells, (E) NK1.1$^+$/CD90.2$^+$ NK T cells. (A-C) N = 6 male mice per group. (D-E) N = 4 female, 3 male mice per group. (F-G) CD3$^+$ cells counted per mm^2 of stroma (F) or tumor nests (G) in immunofluorescence stained pancreas tissues. N = 3 male, 3 female mice per group. (H) representative images of CD3$^+$ T cell infiltration in tumor and associated stroma of OT-PDAC^{parental} (left) and OT-PDAC^{IL6} (right) mice. Tissues were stained with DAPI (blue), CD3 (magenta), and Pancytokeratin (PanCK, green). (scale bars = 100 um) (I) Pathologist-evaluated number of tumor-associated lymphoid aggregates in H&E stained pancreas cross sections from tissue collected at 5 days. N = 3 male, 3 female mice per group. (J) Representative H&E image of lymphoid aggregates adjacent to tumor and stroma in OT-PDAC^{IL6} pancreas (left) and magnified image of lymphoid aggregate (right). Area of magnification is denoted on left image with orange box. Error bars represent SEM. 2-group analysis tested with unpaired t-test. **** $p<0.0001$, *** $p<0.001$, ** $p<0.01$, * $p<0.05$.

Figure 3

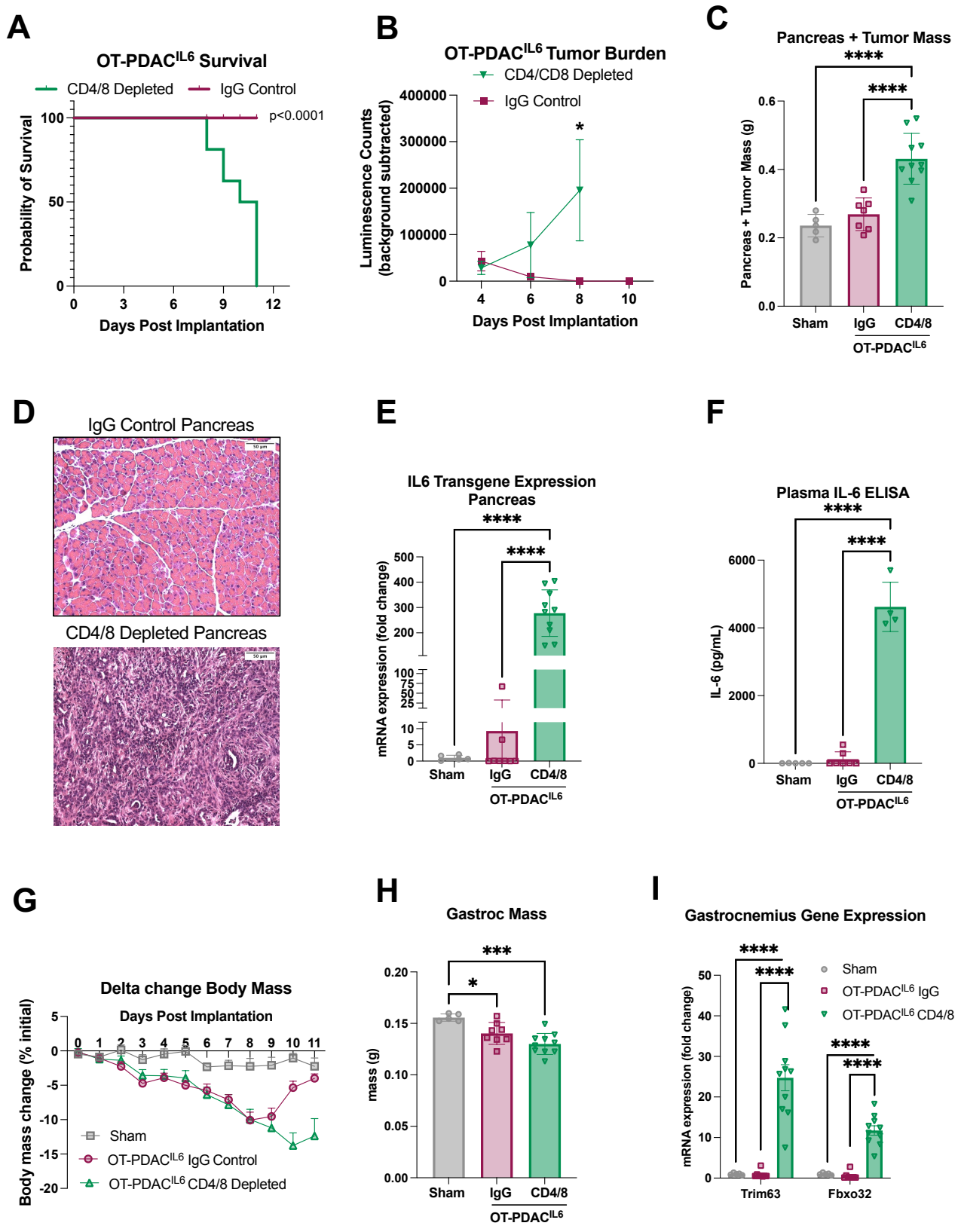

Figure 3: CD4^{+} and CD8^{+} T cells are necessary for OT-PDAC^{IL6} tumor clearance. (A) Survival comparison of OT-PDAC^{IL6} mice given CD4/CD8 depletion or IgG control antibodies. Statistically tested with Log-rank (Mantel-Cox) test. (B) OT-PDAC$^{IL6\text{-}LUC}$ tumor growth, measured by IVIS imaging. Statistically tested with 2-way ANOVA, for time points with representation from both groups, with Šídák multiple testing correction. (C) Pancreas and tumor mass at endpoint. (D) Representative pancreas cross sections at humane euthanasia endpoint from IgG control (top) and CD4/CD8 depleted (bottom) mice. Scale bars represent 100 um. (E) expression of *Il6 transgene* expression, measured by qPCR. (F) Plasma IL6 measured by ELISA. (G) Body mass change as a percentage of initial body mass over time. Statistically tested with Mixed-effects analysis with repeated measures. $p<0.0001$ for Time and Time x Tumor Status. $p=0.0048$ for Tumor Status. (H) Gastrocnemius muscle mass at humane euthanasia endpoint normalized to initial body mass. (I) Atrophy-related gene expression (*Trim63* and *Fbxo32*) in gastrocnemius muscle, measured by qPCR. All male mice, N = 5 sham, 10 PDAC^{IL6} per antibody treatment group. Error bars represent SEM. 3 group studies were statistically tested with a 1-way ANOVA and Tukey correction for multiple comparisons. **** $p<0.0001$, ***$p<0.001$, **$p<0.01$, *$p<0.05$.

Figure 4

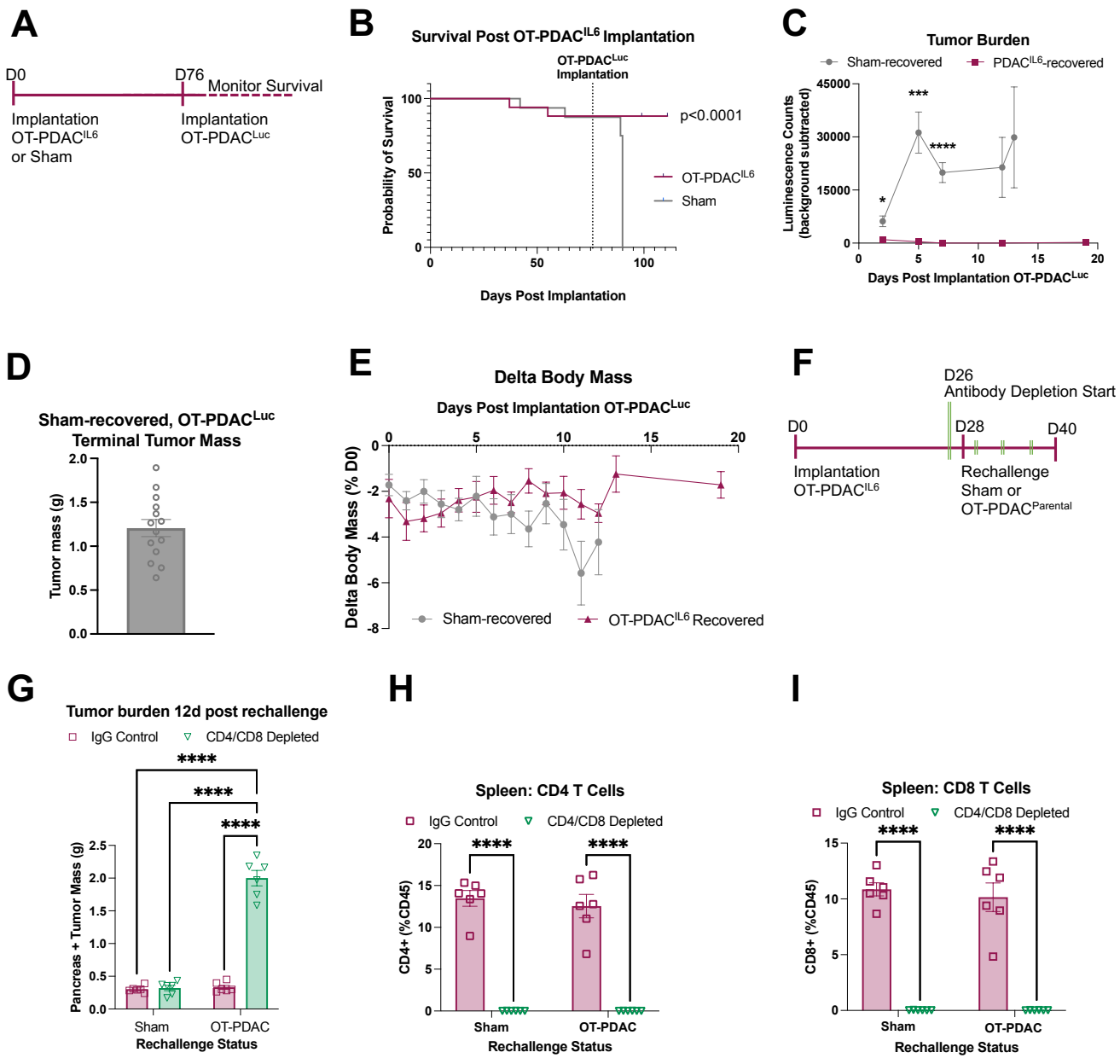

480

481

Figure 4: OT-PDAC^{IL6} induces a durable T cell response to OT-PDAC^{Parental} tumors. (A) Schematic timeline for B-E. Mice were implanted with OT-PDAC^{IL6} or given sham surgery, then all mice were rechallenged with OT-PDAC$^{Parental-LUC}$ after 76 days. (B) Survival comparison of OT-PDAC^{IL6}-recovered and sham-recovered mice. Statistically tested with Log-rank (Mantel-Cox) test. (C) OT-PDAC$^{Parental-LUC}$ tumor growth, measured by IVIS imaging. Statistically tested with mixed effects model and Šídák multiple testing correction, using imputation to match PDAC^{IL6} endpoint with the sham endpoint. (D) Tumor mass at humane euthanasia endpoint for sham-recovered OT-PDAC$^{Parental-LUC}$ tumors. (E) Body mass change as a percentage of initial body mass over time. Statistically tested with mixed effects model and Šídák multiple testing correction at timepoints where both groups were represented. p=0.0435 for Time, p=0.4903 for Tumor Status, p=0.0002 for Time x Tumor Status. (A-E) N = 7 male PDAC^{IL6}, 8 male sham, 7 female PDAC^{IL6}, 6 female sham. (F) Schematic timeline for G-I. Mice were implanted with OT-PDAC^{IL6} or given Sham surgery. 28 days later, mice were rechallenged with OT-PDAC^{Parental}, and given CD4/CD8 depletion or IgG control antibodies beginning on D26 and every 4 days thereafter (denoted with double green lines). (G) Pancreas/tumor mass at 12 days. (H) Intra-tumoral CD4^{+} T cells at 12 days. (I) Intra-tumoral CD8^{+} T cells at 12 days. (F-I) All male mice N = 6 per group. Error bars represent SEM. 2x2 studies were statistically tested with a full effects model 2-way ANOVA and Sidak multiple comparisons test. **** p<0.0001, ***p<0.001, **p<0.01, *p<0.05.